Since January 2020 Elsevier has created a COVID-19 resource centre with free information in English and Mandarin on the novel coronavirus COVID-19. The COVID-19 resource centre is hosted on Elsevier Connect, the company's public news and information website.

Human Pathology (2021) 116, 49–62

ELSEVIER

Human PATHOLOGY

www.elsevier.com/locate/humpath

Original contribution

Distinctive pseudopalisaded histiocytic hyperplasia characterizes the transition of exudative to proliferative phase of diffuse alveolar damage in patients dying of COVID-19☆,☆☆

Michael Kritselis DO[a], Ilyas Yambayev MD[a], Andrey Prilutskiy MD[a], Artem Shevtsov MD, PhD[a], Charitha Vadlamudi MD[a], Hanqiao Zheng MD, PhD[a], Murad Elsadwai MD[a], Lina Ma MD, MS[a], Emily Aniskovich BS[a], Yachana Kataria PhD[a], Sara Higgins MD[a], Carmen Sarita-Reyes MD[a], Tao Zuo MD[a], Qing Zhao MD, PhD[a], Karen Quillen MD[b], Eric J. Burks MD[a,*]

[a] *Department of Pathology & Laboratory Medicine, Boston University School of Medicine, Boston Medical Center, Boston, MA, 02118, USA*
[b] *Department of Hematology and Oncology, Boston University School of Medicine, Boston Medical Center, Boston, MA, 02118, USA*

Received 10 May 2021; revised 21 June 2021; accepted 24 June 2021

Available online 14 July 2021

Keywords:
SARS-CoV-2;
Autopsy;
COVID-19;
Histiocyte;
Multiplex immunohistochemistry

Summary Severe COVID-19 results in a glucocorticoid responsive form of acute respiratory distress (ARDS)/diffuse alveolar damage (DAD). Herein we compare the immunopathology of lung tissue procured at autopsy in patients dying of SARS-CoV-2 with those dying of DAD prior to the COVID-19 pandemic. Autopsy gross and microscopic features stratified by duration of illness in twelve patients who tested positive for SARS-CoV-2 viral RNA, as well as seven patients dying of DAD prior to the COVID-19 pandemic were evaluated with multiplex (5-plex: CD4, CD8, CD68, CD20, AE1/AE3) and SARS-CoV immunohistochemistry to characterize the immunopathologic stages of DAD. We observed a distinctive pseudopalisaded histiocytic hyperplasia interposed between the exudative and proliferative phase of COVID-19 associated DAD, which was most pronounced at the fourth week from symptom onset. Pulmonary macrothrombi were seen predominantly in cases with pseudopalisaded histiocytic hyperplasia and/or proliferative phase DAD. Neither pseudopalisaded histiocytic hyperplasia nor pulmonary macrothrombi was seen in non-COVID-19 DAD cases, whereas microthrombi

☆ Competing interests: None.
☆☆ Funding/Support: This work was supported by the Boston University Mallory Pathology Associates, Inc. and Boston Medical Center.
* Corresponding author. Boston University Mallory Pathology Associates, 670 Albany Street, Suite 304, Boston, MA, 02118, USA.
E-mail address: ejburks@bu.edu (E.J. Burks).

https://doi.org/10.1016/j.humpath.2021.06.008

were common in DAD regardless of etiology. The inflammatory pattern of pseudopalisaded histiocytic hyperplasia may represent the distinctive immunopathology associated with the dexamethasone responsive form of DAD seen in severe COVID-19.

1. Introduction

The global pandemic of severe acute respiratory syndrome coronavirus 2 (SARS-CoV-2) has infected over 155 million worldwide and led to over 3.2 million deaths at the time of this writing [1]. The disease course is highly variable, ranging from asymptomatic carrier [2] to severe viral pneumonia with acute respiratory distress syndrome (ARDS). Subsets of patients with severe illness have viral sepsis [3], cytokine storm [4] and occasionally meet clinicopathologic criteria for hemophagocytic lymphohistiocytosis (HLH) [5]. Part of the spectrum in disease course has been linked to inborn errors in the type I interferon immune pathway [6], as well as the development of neutralizing autoantibodies against type I interferons in a subset of patients [7]. These findings would suggest that immunopathologic differences might be observed between asymptomatic individuals and those with severe COVID-19 disease; a hypothesis that is supported by a randomized control trial in which dexamethasone improved outcome in COVID-19 patients requiring respiratory support [8].

Since the onset of the pandemic, there have been several autopsy series describing the histopathologic features of patients dying with COVID-19 [9−13]. Early results showed typical features of diffuse alveolar damage (DAD) [14,15] and an apparent increase in pulmonary thrombi [16,17]. More recently, a timeline of the usual histopathologic phases of DAD as they progress from exudative, proliferative, and fibrotic stages has been proposed [18], with in situ viral detection generally limited to the exudative phase of the disease [19]. Concordant with these observations, RNA sequencing data have shown marked differences between the immune response in early versus late COVID-19 DAD, which was supported by single-plex immunohistochemistry in subsets of cases [20]. In this study, we seek to (1) further establish the histopathologic timeline of pulmonary findings in patients dying of COVID-19 ARDS while characterizing the immune cell infiltrates using a multiplex (CD4, CD8, CD68, CD20, AE1/AE3) immunohistochemical assay to establish changes in the proportion of lymphocyte subsets and histiocytes over the disease course; (2) quantitate the frequency of microthrombi and macrothrombi; and (3) correlate these findings with non-COVID-19 related DAD controls and patients dying from other causes while having asymptomatic COVID-19 infection.

2. Materials and methods

After obtaining consent from next of kin, an autopsy was performed on twelve consecutive patients testing positive for SARS-CoV-2 nucleic acid on an antemortem upper respiratory swab between April 15 and July 24, 2020. Chart review of the electronic health record was performed to determine age, sex, race, date of symptom onset, date of hospitalization, date and types of treatment, C-reactive protein (CRP), and D-dimer levels throughout the course of hospitalization. Diagnostic SARS-CoV-2 testing was performed by RT-PCR of nasopharyngeal swabs in a CLIA-certified laboratory during hospital admission. The D-dimer assay was serially monitored throughout the hospital course using the IL D-dimer HS assay (Instrumentation Laboratory, Bedford, MA, USA), which is a quantitative immunoturbidimetric assay reported in D-dimer units (DDU). IgG antibody analyses were performed by the clinical pathology laboratory at Boston Medical Center (BMC). Serum samples were run on the Abbott Architect i2000 Instrument using the Abbott SARS-CoV-2 IgG assay per the manufacturer's instructions (SARS-CoV-2 IgG; Abbott Laboratories, Abbott Park, IL). This assay is a chemiluminescent microparticle immunoassay (CMIA) for detection of IgG antibodies in human serum against the SARS-CoV-2 nucleoprotein. Samples were interpreted as positive (index value $\geq$ 1.4) or negative (index value $<$ 1.4) based on the index values reported by the instrument. Qualitative results were used in the analyses. Cases 1 to 4 have been separately reported as manifesting features of SARS-CoV-2 associated hemophagocytic lymphohistiocytosis [5].

The autopsies were performed in a negative pressure room using Personal Protective Equipment (PPE), including an N95 mask and powered air-purifying respirator (PAPR). Harvested organs were thinly sliced, photographed, and fixed for 24 h in 10% neutral buffered formalin (NBF). Four tissue blocks were routinely taken from each lobe of the lung (20 total) and fixed for an additional 6−12 h in 10% NBF before processing. Seven patients dying of diffuse alveolar damage preceding the pandemic (2007−2019) were identified having FFPE lung blocks (median, two per case) available to serve as controls. Hematoxylin and Eosin (H&E) stained sections were prepared and reviewed by two anatomic pathologists (MK and EB). Reviewers were not blinded to the cause of DAD.

Immunohistochemistry was performed using freshly cut 5 μm thick FFPE tissue sections from a lung tissue block

most representative of the overall stage of DAD for the individual patient. The proportion of blocks chosen from right versus left lobes was similar (2:1) between the symptomatic COVID-19 and control group. Single-plex immunohistochemistry was performed on a Ventana Benchmark Ultra (Roche, Tucson, AZ) using a rabbit polyclonal antibody against the SARS-CoV Nucleocapsid protein (NB100-56576: Novus Biologicals, Centennial, CO) incubated for 36 min at 1:400 dilution after heat-induced epitope retrieval for 32 min at 95 °C using alkaline buffer (CC1, #950-124, Ventana). Slides were visualized with Optiview detection (#760-700, Ventana). Multiplex immunohistochemistry was performed using the Ventana Discovery-Ultra platform (Roche, Tucson, AZ) using pre-diluted antibodies directed against CD8 (clone: SP57, 790-4460; Roche), CD68 (clone: KP-1, 790-2931; Roche), CD20 (clone: L26, 760-2531; Roche), Pan Keratin (clone: AE1/AE3/PCK26, 760-2595; Roche), CD4 (clone: SP35, 104R-18; Cell Marque) after heat-induced epitope retrieval for 32 min at 95 °C using alkaline buffer (CC1, #950-124, Ventana). Primary antibody detection was performed using Discovery Hapten Detection with Discovery Anti-Mouse HQ (#760-4814, Ventana), Discovery Anti-Mouse NP (#760-4816, Ventana), and Discovery Anti-Rabbit HQ (#760-4815, Ventana), and visualized with Ventana chromogens: DAB, #760-124; Purple, #760-229; Green, #760-271; Yellow, #760-239; Teal, #760-239. Primary antibody inactivation for the multiplex reactions was carried out using temperature-induced denaturation for 8 min at 95 °C with CC2 buffer (#950-123, Ventana). Internal and on-slide external controls (Tonsil/Appendix) were examined for each slide and judged satisfactory before interpretation.

The Institutional Review Board reviewed this study and waived jurisdiction.

3. Results

3.1. Patient characteristics

Clinical features of SARS-CoV-2 positive patients are summarized in the Table. Twelve patients tested positive by PCR on nasopharyngeal swabs prior to death. Ten of these were symptomatic from COVID-19 prior to death, while two patients were asymptomatic, dying of unrelated causes. Symptomatic patients were older (median age 69.5 years) than those who were asymptomatic (median age 51.5 years), and 8/10 (80%) self-identified as black. Seven patients received biological agents as part of their treatment prior to death. Anakinra, a human interleukin-1 receptor antagonist, was administered to two patients who received 6 doses of 100 mg IV over 3 days, which was completed 9 and 85 days prior to death. Sarilumab, a human monoclonal interleukin-6 inhibitor, was administered to 5 patients as a single dose of 200 mg IV, which was completed in a

Table Clinicopathologic features.

	Demographics				Clinical Parameters			Duration (days)			Treatment		Relevant Comorbidities						Lung Weight		Pathologic Features						
Case No.	Age	Sex	Race	Presentation	Temperature (Max, F)	Upper Respir. PCR	D-dimer Max. (ng/mL DDU)	Symptoms	Hospitalization	Intubation	Biologic Treatment	Heparin	Obesity	Hypertension	Diabetes	Heart Disease	Kidney Disease	Lung Disease	Right (grams)	Left (grams)	Exudative DAD	Proliferative DAD	Recovered DAD	Pseudopalisaded Histiocytic Hyperplasia	Microthrombi	Macrothrombi	SARS IHC lung
1	91	M	AA	C,D,F	102.8	+	1929	8	7	NI	-	L	+	+	-	+	+	-	750	512	+	-	-	-	-	-	+
2	72	M	AA	C,D,F	101.3	+	26277	6	3	NI	S	L	-	+	-	+	+	-	950	750	+	-	-	-	+	-	+
3	64	F	AA	C,D,F	102.7	+	69000	15	10	3	S	L/U	+	+	+	-	+	-	740	630	+	+	-	+	+	+	+
4	72	M	CA	C,F	104.0	+	541	18	14	11	A	L	+	+	+	+	+	-	1242	1107	+	-	-	-	+	-	+
5	36	F	H	D,F	103.5	+	3937	23	16	16	-	L/U	+	-	-	-	-	+	970	1060	+	+	-	+	-	+	+
6	73	F	AA	D,F	102.3	+	9655	27	25	25	S	L	+	+	+	+	-	-	1050	850	-	+	-	+	+	-	-
7	67	M	AA	C,D,F	103.0	+	15448	31	20	18	S	L	-	+	+	-	+	-	1240	1050	+	+	-	+	+	+	-
8	78	F	AA	D,F	102.9	+	44434	38	35	32	-	L	-	+	+	-	-	-	878	697	+	+	-	-	+	+	-
9	63	M	AA	C,D,F	101.2	+	28508	41	30	28	S	L	-	+	-	-	-	+	1480	1250	-	+	-	+	-	-	-
10*	61	F	AA	C,D,F	101.8	+	2861	92	92	74*	A	U	+	+	+	+	+	+	440	375	-	-	+	-	-	-	-
11	65	M	H	Stg IV SCLC	99.8	+	4908	..	8	NI	-	L/U	-	-	-	-	-	-	649	554	-	-	-	-	-	-	+
12	38	M	CA	Hemorrhage	99.6	+	2521	..	5	1	-	-	-	-	-	+	-	-	1063	558	-	-	-	-	-	-	-
13	55	F	CA	MI, HLH	..	..	..	..	5	1	..	..	-	+	+	+	-	-	660	590	+	-	-	-	+	-	..
14	51	F	CA	..	99.1	..	..	..	15	1	..	..	+	+	+	-	-	-	1000	900	+	-	-	-	+	-	..
15	60	F	CA	Cancer	..	..	..	..	16	8	..	..	+	-	-	-	-	-	..	1360	+	-	-	-	-	-	..
16	45	F	AA	AIDS, Infection	102.1	..	16985	..	18	18	..	..	+	+	-	-	-	+	1400	1600	-	+	-	-	-	-	..
17	61	M	CA	Cancer	103.4	..	..	..	21	19	..	..	+	+	-	-	-	-	1240	1070	-	+	-	-	+	-	..
18	67	M	CA	Cancer	101.7	..	720	..	51	6	..	..	-	-	-	-	-	-	900	925	-	+	-	-	-	-	..
19	27	F	AA	SLE, Infection	..	..	..	..	75	..	..	..	-	+	-	-	+	-	1150	1000	-	+	-	-	-	-	..

Abbreviations: AA, African American; CA, Caucasian; H, Hispanic; C, cough; D, dyspnea; F, fever; MI, myocardial infarction; HLH, hemophagocytic lymphohistiocytosis; NI, not intubated; S, Sarilumab; A, Anakinra; L, low-molecular weight heparin; U, unfractionated heparin; CRP, C-reactive protein; .., unknown or not tested. *Patient 10 was symptomatic of covid and intubated 74 days prior to death but was extubated 37 days prior to death, discharged and ultimately readmitted 1 month later with encephalitis which led to her demise. She died with symptoms unrelated to pulmonary COVID-19 infection.

median of 20 days (range 2−29 days) prior to death. Seven patients dying of diffuse alveolar damage preceding the pandemic (2007−2019) were identified having FFPE tissue available to serve as controls. The median age was 55 years with a male to female ratio of 2:5 and a minority who were black (2 of 7). There were diverse and overlapping disease states associated with DAD in these patients, including cancer (pheochromocytoma, esophageal, and lung carcinomas) undergoing multiple treatments (surgery, radiation, chemotherapy), immune disorders (SLE, HLH, and AIDS), and infections (cryptococcal meningitis, Pneumocystis pneumonia, and fungal sepsis).

3.2. Pulmonary immunopathologic findings

3.2.1. Patients dying early without mechanical ventilation

Two patients (cases 1 and 2) died of COVID-19 after the first week of symptom onset (6−8 days) without mechanical ventilation. Both patients had dyspnea and hypoxia but were not intubated due to advanced age and co-morbidities. The lungs were heavy in both patients (right 750−950 gm and left 512−750 gm). Fig. 1 shows the gross and histologic findings. Grossly the lungs showed patchy areas of consolidation, which were edematous and firm. Histologic findings were that of an early exudative phase of DAD, being dominated by alveolar edema, pneumocyte sloughing, and foci of early hyaline membrane formation. One of the two cases showed focal squamous metaplasia. SARS immunohistochemistry was positive multifocally in aggregates of epithelioid cells in both patients. Multiplex immunohistochemistry showed numerous CD68 macrophages and CD4 positive T-cells admixed with sloughed AE1/AE3 positive pneumocytes but only scattered CD8 positive T-cells and rare CD20 positive B-cells.

3.2.2. Patients dying with mechanical ventilation

Seven patients (case 3−9) died while being mechanically ventilated (median 18 days, range 3−32) at a median of 27 days (range 15−41 days) from symptom onset. The lungs were heavier than those dying earlier, with median weights of 1050 gm for right (740−1480 gm) and 1050 gm for left (630−1250 gm). Hyaline membranes were well developed by the third week of infection (Fig. 2) and associated with a variably prominent infiltrate of CD68 positive macrophages with an equal distribution of CD4 and CD8 positive T-cells and infrequent CD20 positive B-cells. By the fourth week of infection (Fig. 3), histiocytes became more numerous, lining distended alveolar ducts forming pseudopalisades with admixed giant cells surrounding fibrinoid debris in a garland-like distribution. This finding was most extensive in cases 6 and 7 in which 70% and 80% of the tissue sections were involved from all five lobes of the lung. Conversely, the extensive histiocytic hyperplasia was limited to a single lobe of the lung (left upper lobe) in patient 5, involving only 10% of tissue blocks examined, and was limited to the bilateral upper and right middle lung lobes of patient 9, where it was present in 45% of the tissue blocks examined. Grossly, the lungs demonstrating this pattern of pseudopalisaded histiocytic hyperplasia showed a more confluent tan-white consolidation. The proliferative phase of DAD (Fig. 4) began at the fourth week and was most prominent during the fifth week postsymptom onset. The gross appearance exhibited a pseudonodular parenchyma with erythematous septa surrounding the alveolar lobules, which were pale tan. Histologically, an interstitial fibroblastic proliferation exhibited a 'tissue culture'-like quality with numerous extravasated red cells and concurrent alveolar pneumocyte hyperplasia. In two cases, concurrent foci of organizing pneumonia characterized by plugs of fibroblasts filling alveolar ducts were observed. SARS immunohistochemistry was not detected beyond the fourth week of symptom onset, with less staining in lungs showing early changes of proliferative phase DAD than those with purely exudative phase DAD (Table). Control patients dying with DAD prior to the COVID-19 pandemic were compared to patients dying of SARS-CoV-2, matching them by time from intubation. The tempo of histologic and immunophenotypic changes was similar with the exception that none of the control cases exhibited the pseudopalisaded histiocytic hyperplasia seen most prominently at the fourth week postsymptom onset in those dying of SARS-CoV-2.

3.2.3. Patient dying after extubation from another cause

One patient (Case No. 10) died 37 days after extubation (92 days after symptom onset) as a result of autoimmune encephalitis. Lung weights were only slightly above normal (right 440 gm and left 375 gm versus normal female 340 gm and left 299 gm). Fig. 5 shows the gross and histologic features. The gross appearance was congested and red but without discrete foci of consolidation. Histologically, the interstitium showed mild expansion of loose fibrous tissue, dilated capillaries, and minimal chronic inflammation. No other hallmarks of interstitial lung disease such as collagenous fibrosis, microcystic honeycombing, traction bronchiectasis, or vascular changes were observed. Multiplex immunohistochemistry showed scattered interstitial lymphocytes with an admixture of CD4 and CD8 positive cells. AE1/AE3 highlighted an intact layer of pneumocytes, and CD68 positive histiocytes had decreased to near-normal levels. SARS immunohistochemistry was negative.

3.2.4. Patients dying with COVID-19 but from other causes

Two patients tested positive for SARS-CoV-2 by RT-PCR on admission and on the day preceding death with no COVID symptoms. Both patients were also positive for IgG and IgM SARS-CoV-2 antibodies in their serum within 3 days of the death, indicating the asymptomatic period was long enough to mount an immune response against the

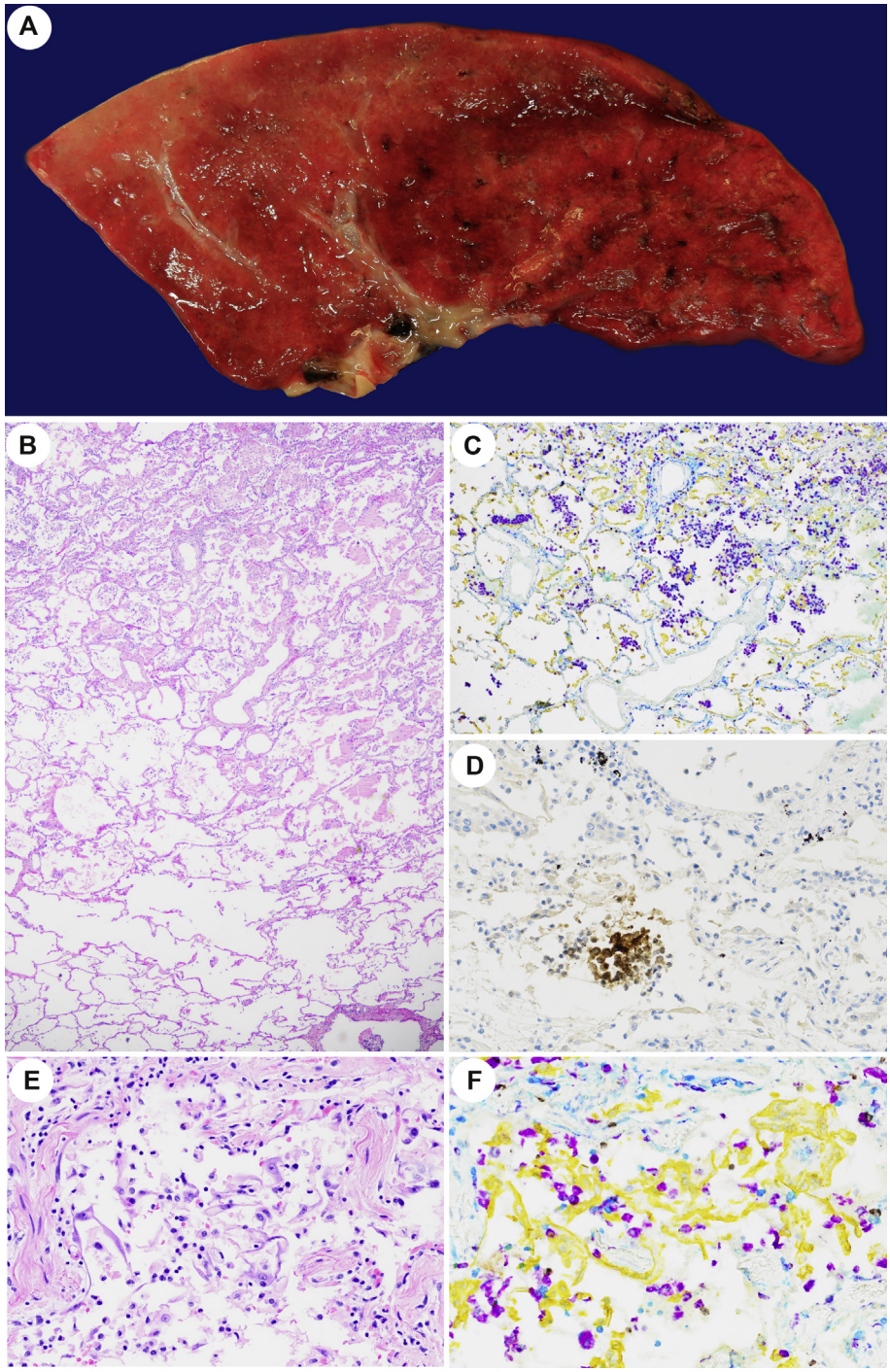

Fig. 1 Pulmonary Findings in Patients Dying of SARS-CoV-2 during the first/second week of infection. (A) Grossly, the lungs showed patchy areas of consolidation characterized by a firm edematous cut surface (left) juxtaposed with typical parenchyma that deflates after cutting (right). (B) H&E showing the transition from normal lung (lower left) to regions of pulmonary edema with the alveolar accumulation of disaggregated mononuclear cells (upper right) (40 ×). (C) Multiplex immunohistochemistry from the same region in (B), showing the admixture of sloughed pneumocytes staining with AE1/AE3 (yellow), CD68 positive macrophages (purple), and CD4 positive T-cells (teal). CD8 positive T-cells (brown) are infrequent, and CD20 positive B-cells (green) were rare and not visualized in this figure (100 ×). (D) SARS immunohistochemistry showing staining in a cluster of epithelioid cells (200 ×). (E) H&E and (F) multiplex immunohistochemistry from the same region showing an admixture of sloughed pneumocytes staining with AE1/AE3 (yellow), CD68 positive macrophages (purple), and CD4 positive T-cells (teal). CD8 positive T-cells (brown) are infrequent, and CD20 positive B-cells (green) were rare and not visualized in these figures (200 ×).

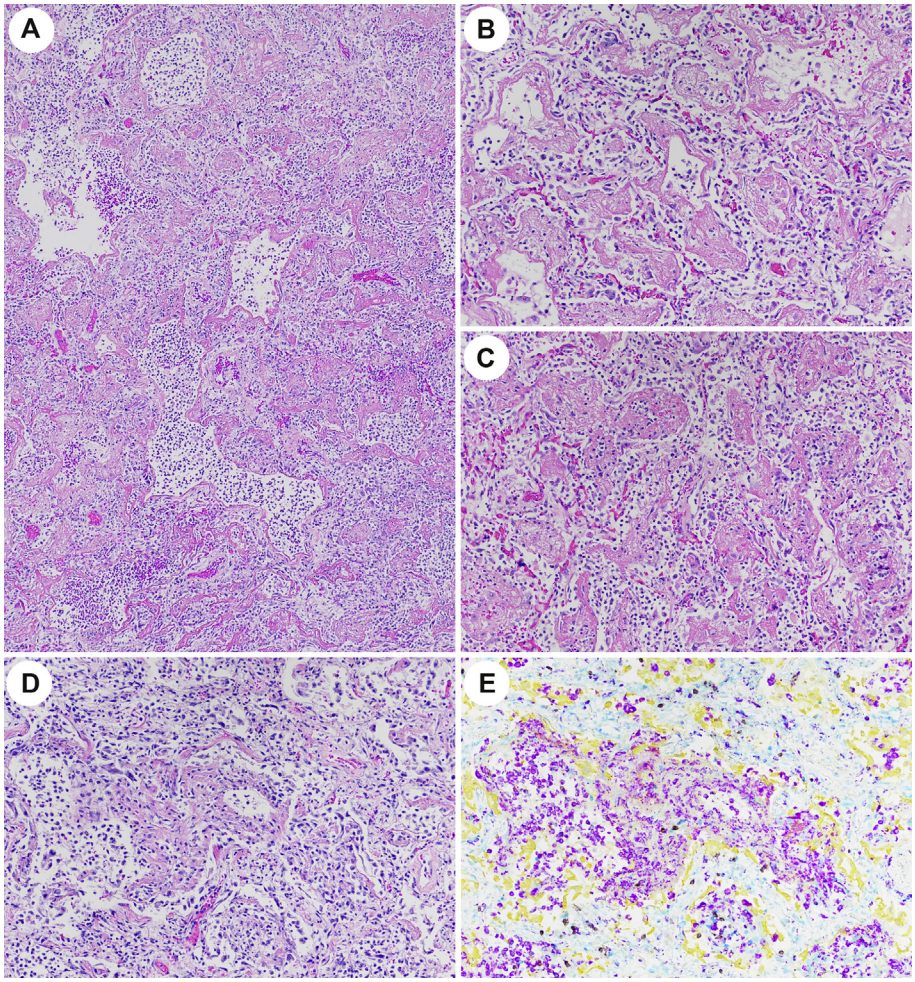

Fig. 2 Pulmonary Findings in Patients Dying of SARS-CoV-2 during the third week of infection. (A–C) H&E (40 × and 200 ×) focally showing hyaline membranes coalescing (C) to resemble acute fibrinous organizing pneumonia (AFOP). Paired H&E (D) and multiplex immunohistochemistry (E) showing the mononuclear infiltrate within partially organizing hyaline membranes with numerous CD68 positive macrophages (purple) with admixed CD4 (teal) and CD8 (brown) positive T-cells, sloughed AE1/AE3 (yellow) positive pneumocytes and rare to absent CD20 (green) positive B-cells (200 ×).

virus. In one case (case 11), the cause of death was spontaneous tumor lysis associated with metastatic cancer, while the other patient (case 12) died from a ruptured mesenteric artery with hemoperitoneum. Histologic features typical of SARS-CoV-2 were seen in only one patient (case 11, Fig. 6), dying of stage IV small cell lung carcinoma prior to initiation of treatment. The lungs in this patient were mildly enlarged (right 649 gm and left 554 gm) with small foci of white-tan consolidation comprising less than 5% of the lung volume, in addition to being involved by metastatic small cell carcinoma. Histologically the consolidated foci were characterized by alveolar edema, with hyaline membranes, and pneumocyte sloughing with prominent intra-alveolar admixtures of CD68 positive histiocytes and CD4 positive T-cells, only scattered CD8 positive T-cells, and few to none CD20 positive B-cells. SARS immunohistochemistry showed focal staining in alveolar pneumocytes. The second patient (case 12) showed multiple septic emboli in the lungs secondary to infectious endocarditis, but no histologic features typical of SARS-CoV-2 pneumonitis were observed, and SARS immunohistochemistry was negative in the lung tissue.

3.3. Frequency of pulmonary thrombi and infarction

Pulmonary microthrombi (Fig. 7E–F) were observed in 6 of the 10 patients (60%) with symptomatic SARS-CoV-2 infection in comparison to 3 of 7 patients (43%) dying with DAD from causes unrelated to COVID-19 pre-pandemic (Table). Conversely, macrothrombi (Fig. 7A–D) were observed in 4 of 10 patients (40%) dying of SARS-CoV-2 but in none of the non-COVID DAD cases. D-dimer levels were elevated in all patients dying of COVID-19

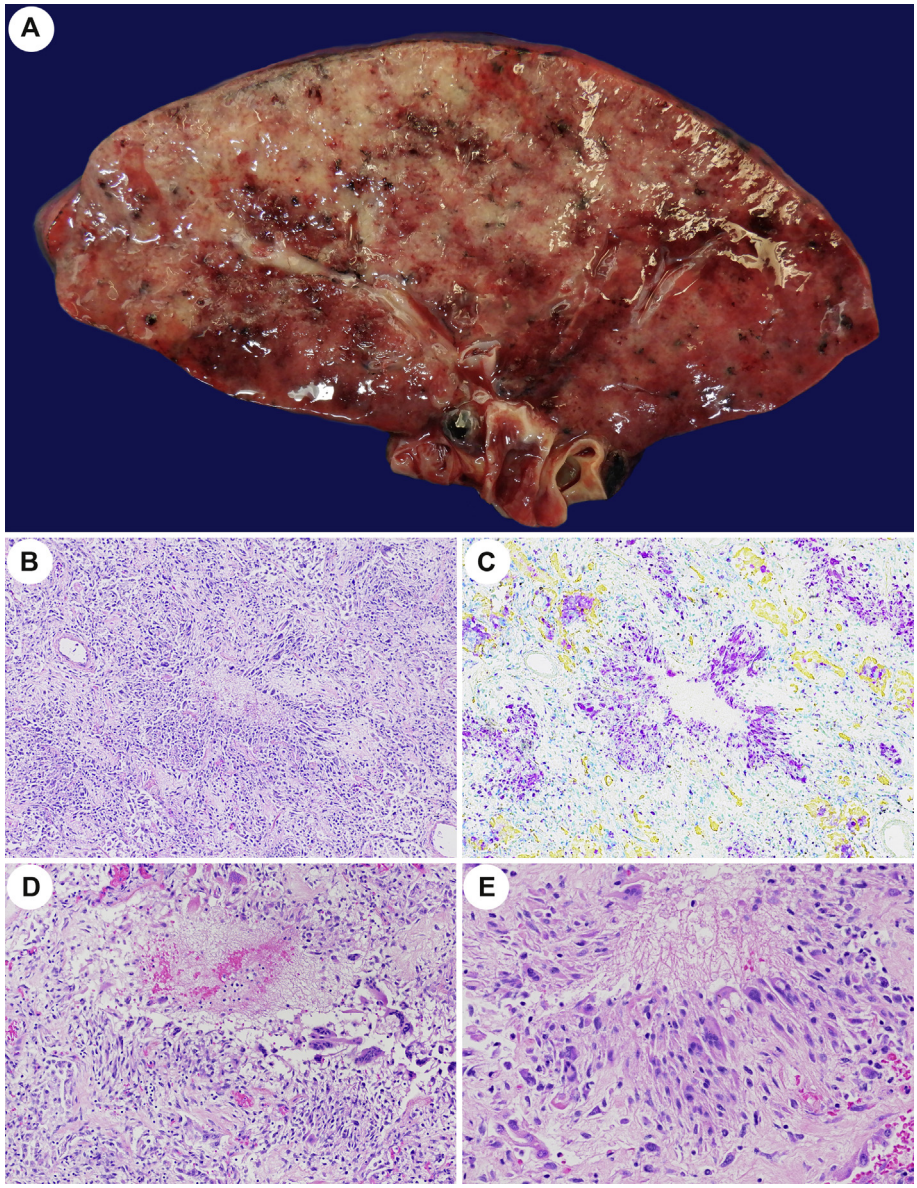

Fig. 3 Pulmonary Findings in Patients Dying of SARS-CoV-2 the fourth week of infection. (A) Gross figure of lung showing firm tan-white regions of consolidation with punctate foci of hemorrhage. (B) H&E stain (40 ×) and (C) multiplex immunohistochemistry (40 ×) showing prominent histiocytic reaction staining with CD68 (purple) outlining alveolar ducts and alveoli in the typical distribution of hyaline membranes with complete loss of AE1/AE3 (yellow) positive pneumocytes in the same regions. CD4 positive T-cells (teal) are increased both within the histiocytic aggregates, as well as the lung interstitium with fewer CD8 (brown) and rare CD20 (green) positive lymphocytes. (D/E) H&E showing pseudopalisading of histiocytes and multinucleated giant cells in a garland-liked distribution along alveolar ducts devoid of epithelium and surrounding fibrinoid luminal debris. (D 100 × and E 200 ×).

(Table), but values were generally higher in those with macrothrombi (median 29,941 ng/mL DDU) compared to those without (median 6258 ng/mL DDU). Among patients with macrothrombi, only one patient had extrapulmonary thrombosis manifesting as basal ganglia stroke (case 3), and this patient also had the highest D-dimer level (69,000 ng/mL DDU). Areas of pulmonary hemorrhage and infarct were occasionally observed adjacent to macrothrombi (Fig. 7A).

4. Discussion

Herein we describe the gross, histologic, and immunopathologic pulmonary features in a series of 10 patients dying at differing time points following symptomatic COVID-19 and compare these with seven patients dying from DAD/ARDS prior to the COVID-19 pandemic. We further observe two patients dying from other causes with asymptomatic SARS-CoV-2 infection. We establish an

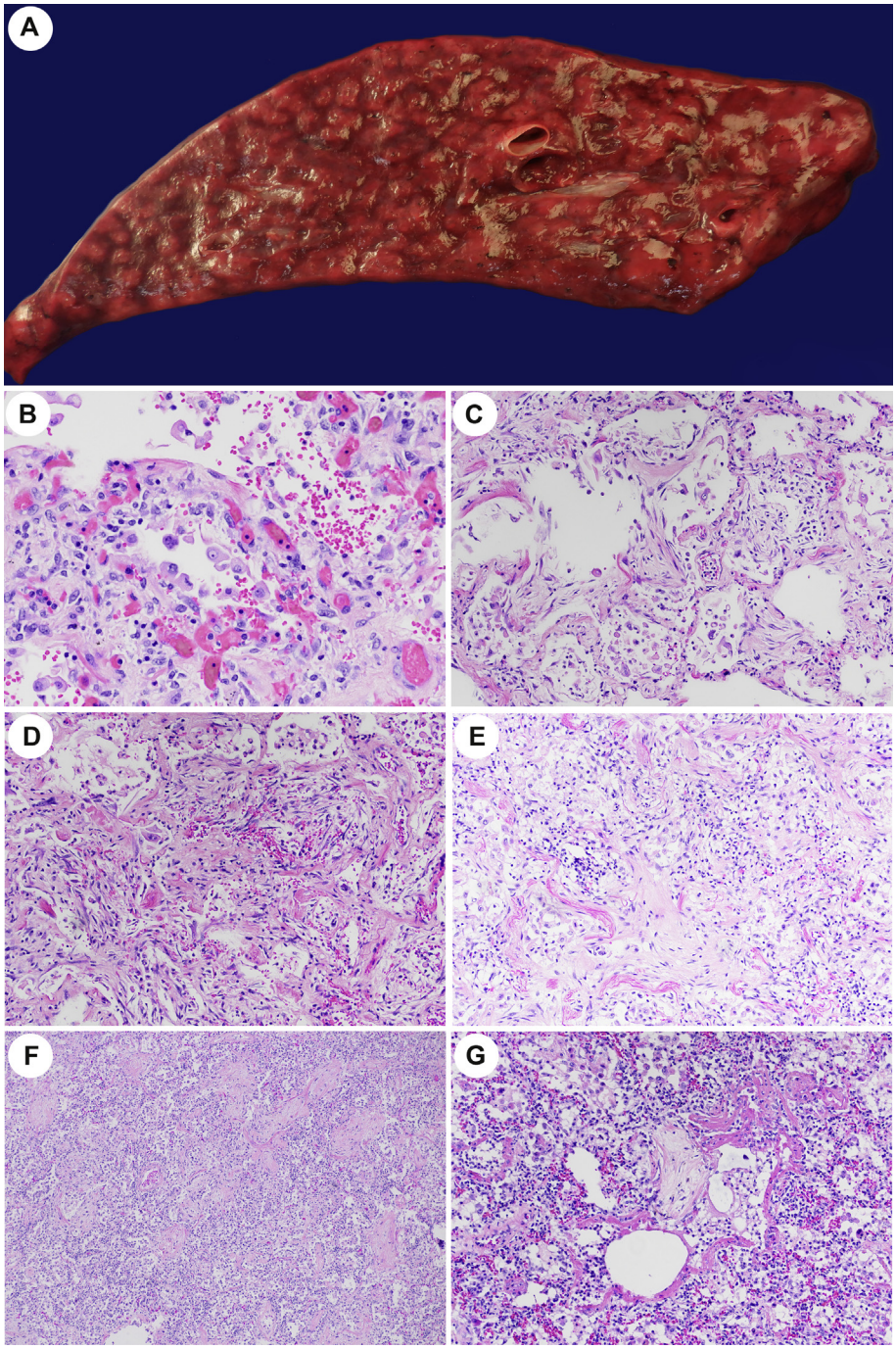

Fig. 4 Pulmonary Findings in Patients Dying of SARS-CoV-2 the fifth week of infection. (A) Gross figure of lung showing a nodular appearance accentuating pale lobules with beefy red septa. (B) H&E showing pneumocyte hyperplasia with early interstitial fibroblastic proliferation (200 ×). (C—E) H&E showing more developed interstitial fibroblastic proliferation with a 'tissue culture'-like quality and extravasated red cells, focally compressing alveoli (E) and producing a solid alveolus (100 ×). (F) An organizing pneumonia pattern characterized by fibroblastic plugs arranged in linear arrays (40 ×) concurrent with (G) foci of hyaline membrane formation (100 ×) was seen in occasional cases.

immunopathologic time sequence and note a unique inflammatory pattern characterized by a pseudopalisaded histiocytic hyperplasia developing between the exudative and proliferative phases of DAD in SARS-CoV-2 but not in control cases of DAD.

Diffuse alveolar damage histologically has sequential exudative, proliferative, and fibrotic phases [21]. The exudative phase is characterized by cell-mediated destruction of the alveolar/endothelial structure leading to leakage of plasma and cellular content into the interstitium

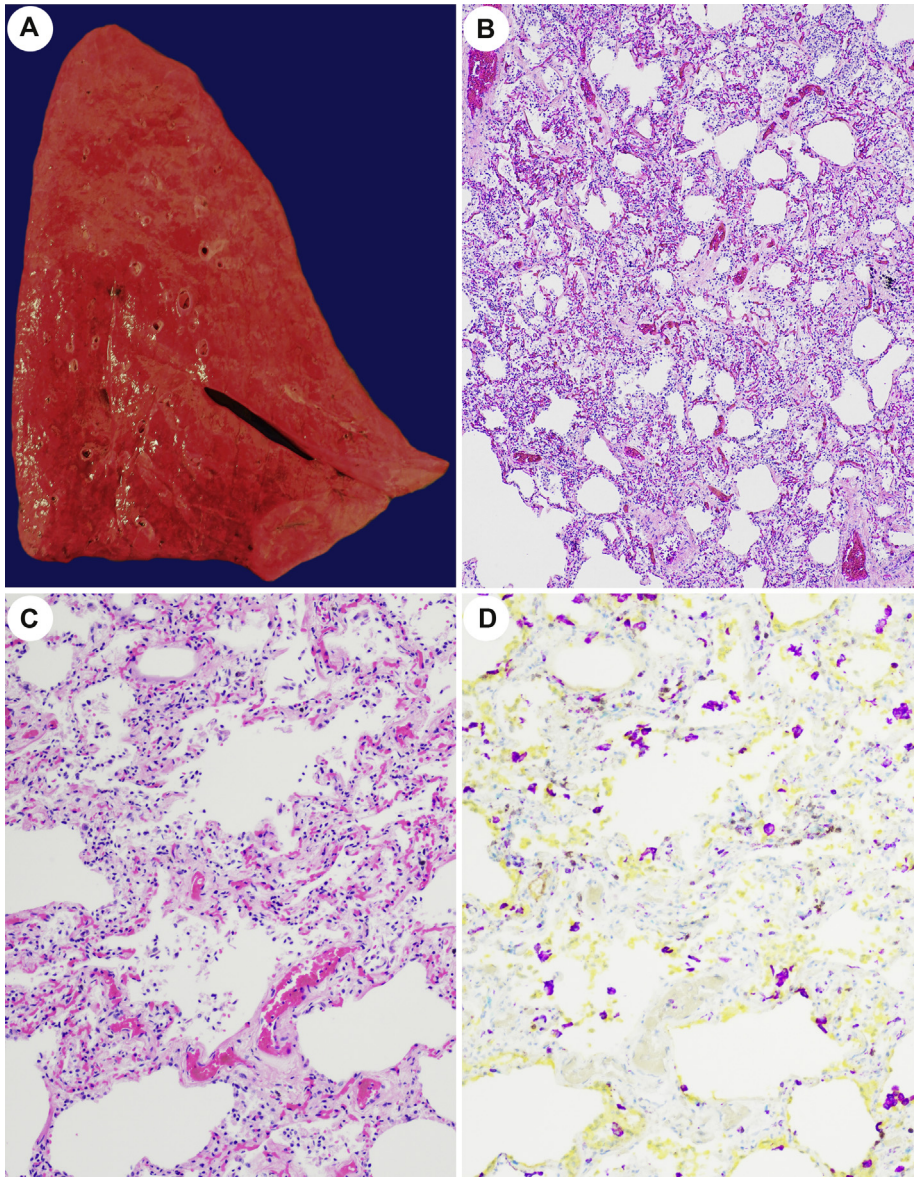

Fig. 5 Pulmonary Findings in Patients Dying after Recovery from SARS-CoV-2 one month after extubation. (A) Gross figure of lung showing mild congestion without discrete foci of consolidation. (B/C) H&E showing minimal residual interstitial expansion by loose fibrous tissue, dilated capillaries, and minimal chronic inflammation (100 × and 200 ×). Multiplex immunohistochemistry showing scattered interstitial lymphocytes are an admixture of CD4 (teal) and CD8 (brown) positive T-cells. AE1/AE3 (yellow) highlights an intact layer of pneumocytes while CD68 (purple) positive histiocytes have decreased to near normal levels (200 ×).

and air space. We observed these features in those dying at 6–18 days from symptom onset, in particular in those dying without mechanical ventilation. Subsequently, the protein and cellular debris organize into hyaline membranes, which was most confluent at the third week post-symptom onset. This is followed by the proliferative phase of DAD characterized by a pneumocyte hyperplasia, attempting to restore the epithelial layer and a myofibroblastic proliferation within the interstitium with morphologic features typical of connective tissue repair. The proliferative phase was observed most prominently in week 4–5 postsymptom onset and only in those who had received mechanical ventilation, usually for at least 3 weeks duration. Finally, a fibrotic phase inconsistently develops as a consequence of failure to resorb collagen deposited during the proliferative phase leading to chronic interstitial fibrosis. We observed only a single patient who had recovered from severe COVID-19 respiratory infection, 3 months after symptom onset and 1 month since mechanical ventilation, who then died of nonpulmonary causes. Lung weights had returned to near normal, and there was only a minimal residual interstitial expansion of loose fibrous tissue and scattered chronic inflammatory cells. Typical hallmarks of interstitial lung disease

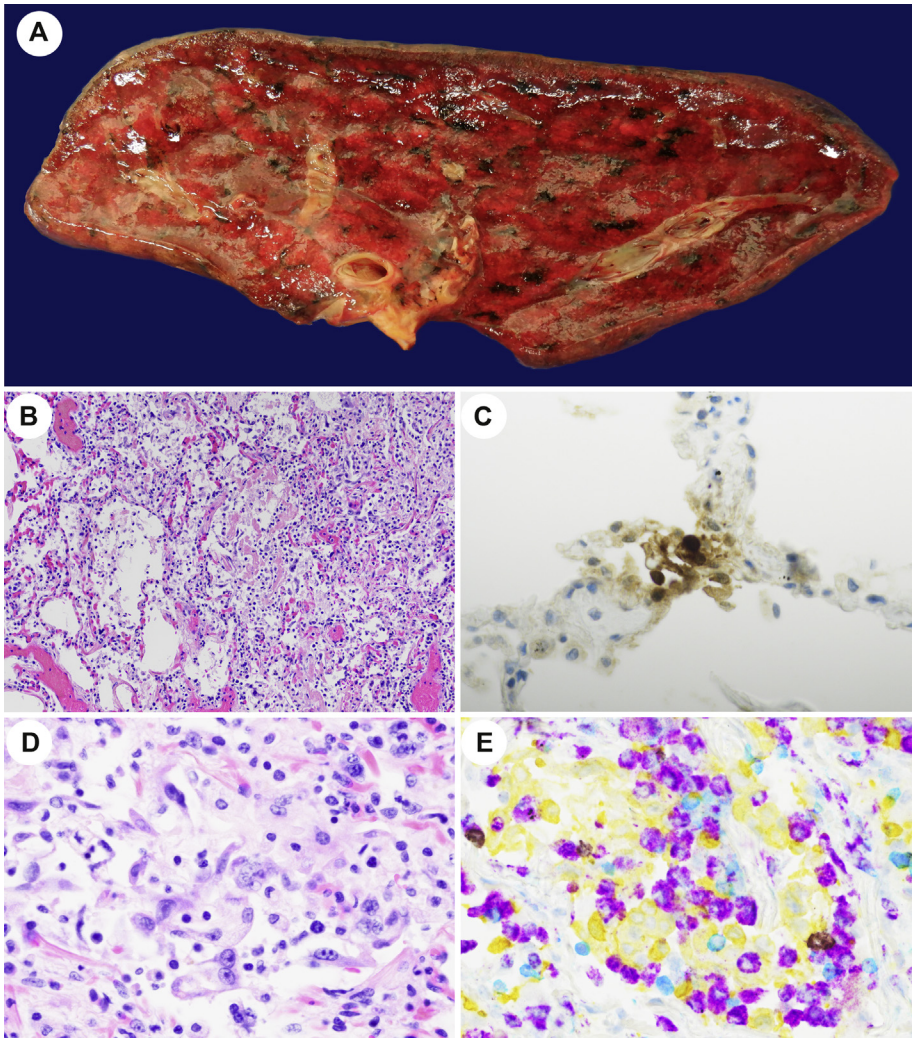

Fig. 6 Pulmonary Findings in Patients Dying from Stage IV Small Cell Lung Cancer with Asymptomatic SARS-CoV-2 Infection. (A) Gross figure of lung showing minimal (~5% of lung parenchyma) patchy pale areas of consolidation. (B) H&E focal hyaline membrane formation with an accumulation of alveolar mononuclear inflammation (200 × and 100 ×, respectively). (C) Immunohistochemistry for SARS-CoV-2 nucleocapsid protein showing focal staining in alveolar pneumocytes (200 ×). (D/E) Paired H&E and multiplex immunohistochemistry showing a predominance of CD68 (purple) positive histiocytes and CD4 (teal) positive T-cells interspersed with sloughed AE1/AE3 (yellow) positive pneumocytes. CD8 (brown) positive lymphocytes are few, while CD20 (green) positive lymphocytes are inconspicuous (400 ×).

(collagenous fibrosis, microcystic honeycombing, traction bronchiectasis, vascular changes) were not observed [22]. The timing of these morphologic phases in SARS-CoV-2 associated DAD is in keeping with the timeline proposed in a recent systematic review of the pathologic findings from 131 postmortem lung samples taken from patients dying from COVID-19 [18].

Using multiplex immunohistochemistry, we were able to characterize the inflammatory infiltrate within each of the phases of DAD and observed the predominant immune cell types were CD68 positive histiocytes and CD4 positive T-cells throughout each phase with relatively fewer CD8 positive T-cells and sparse CD20 positive B-cells. We observed a previously undescribed pattern of inflammation, which was most pronounced during the fourth week from symptom onset (third week of mechanical ventilation) in which striking histiocytic hyperplasia lined the alveolar ducts in a garland-like pseudopalisaded pattern. This was distinct from the loose clusters of histiocytes admixed with sloughed pneumocytes observed in the early exudative phase (first/second week of symptom onset). Recent targeted RNAseq data from lung tissue obtained from sixteen COVID-19 autopsies revealed two distinct immunopathologic profiles [20]. The first was seen in patients dying early (1st week of hospitalization) and was characterized by high interferon stimulating genes, high viral titer, and lower immune cell infiltration. This was in contrast to those dying later (2nd week of hospitalization) in which low interferon

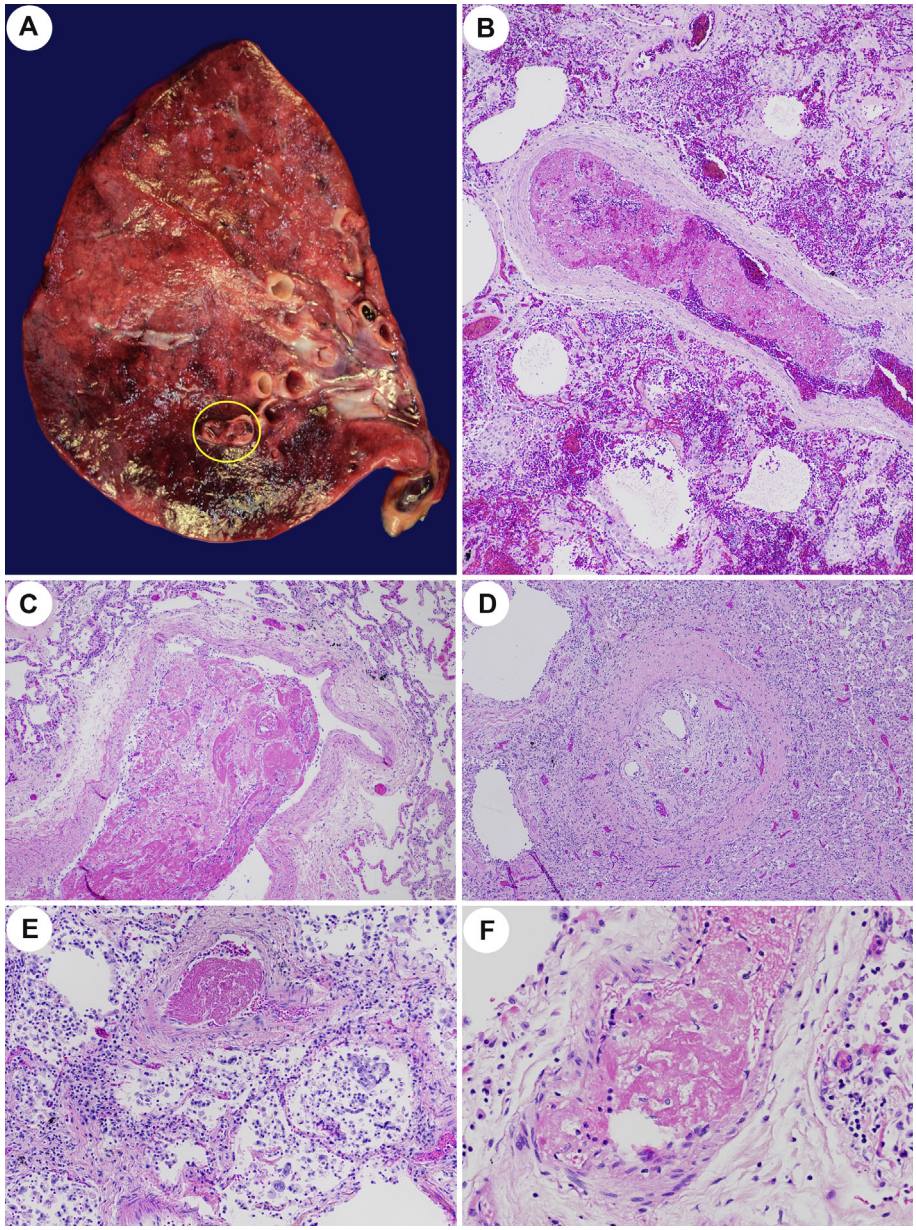

Fig. 7 Pulmonary Findings in Patients Dying of SARS-CoV-2 with Thromboemboli. (A) Gross figure of lung showing a hemorrhagic pulmonary infarct with associated macrothrombus (yellow circle). (B/C) H&E showing histologic features of acute macrothrombi and (D) an organizing thrombus (40 ×); only observed in SARS-Cov-2 associated DAD (40%). (E/F) H&E showing microthrombi commonly seen in both SARS-CoV-2 associated (60%) and in non-SARS-CoV-2 (43%) DAD (200 × and 400 ×, respectively).

stimulating genes, low viral titer, and high immune cell infiltration along with genes associated with tissue regeneration were observed [20]. More recently, investigators using imaging mass cytometry with metal-labeled antibody panels comprised of 36 antibodies showed distinctive phenotypes of myeloid populations in lungs of patients dying of COVID-19 [23]. Specifically, those dying early of disease had alveolar monocytes expressing high IL1β while those dying with late COVID-19 had prominent interstitial macrophages staining with CD14, CD16, CD206, CD163, and CD123.

While our multiplex panel is more limited in scope, the distribution of the pseudopalisaded histiocytes and timing between hyaline membrane prominence of the exudative phase and onset of typical histologic features of proliferative phase DAD leads us to believe that this likely reflects an exaggerated histiocytic reaction associated with resorption of hyaline membrane material. This pattern may be more common in COVID-19 DAD as we did not observe it in our relatively small number of non-COVID-19 DAD control cases. Older light and electron microscopy studies of the organizing/proliferative phase of DAD, prior to the

COVID-19 pandemic, describe the process of re-epithelialization of alveolar lumina with the incorporation of the cellular debris of hyaline membranes along with denuded alveolar epithelial basal laminae to form a 'new' alveolar septum [24]. While scattered luminal and septal inflammatory cells were commonly observed, garland-like arrangements of pseudopalisaded histiocytes have not been described previously in DAD to our knowledge.

It is interesting in the context of this distinctive inflammatory pattern that the RECOVERY collaborative group showed dexamethasone reduced 28-day mortality in patients with COVID-19 who required mechanical ventilation when given after the first week of illness but had no effect in patients not receiving respiratory support [8]. The authors of this study suggested that the stage of disease in which therapy was initiated was likely dominated by immunopathological elements, with active viral replication only playing a secondary role. To this point, we observed maximal immunohistochemical viral detection in the preceding exudative phase with limited to absent staining upon advancement to proliferative phase, a finding confirmed by other groups, as well [19]. As such, the pseudopalisaded histiocytic hyperplasia observed in our series correlates well with the timing of the observed mortality benefits demonstrated in the RECOVERY dexamethasone trial, corresponding to a time when in situ viral detection is diminishing. None of the patients in our series received dexamethasone as they presented prior to the results of the RECOVERY trial. Current clinical guidelines recommend glucocorticoids be administered to patients with early, moderate to severe ARDS and those precipitated by a steroid-responsive process [25]. Glucocorticoids are generally not recommended for patients with mild ARDS, late-stage disease (beyond 14 days) [26], or in patients whose ARDS was precipitated by a viral infection such as influenza as their use has been associated with worse outcomes [27,28]. A more recent meta-analysis, however, is challenging these guidelines, suggesting that corticosteroids probably reduce mortality in patients with ARDS regardless of whether COVID-19 was the inciting agent [29]. A further confounding factor in our conclusion is that four of the five patients with the pseudopalisaded histiocytic reaction were also treated with sarilumab a median of 20-days prior to death to manage cytokine release syndrome [30]. Sarilumab is a monoclonal antibody inhibitor of IL-6 that is produced by innate immune cells, such as monocytes/macrophages, as part of the host defense against infectious agents [31], and thus, we cannot exclude that the pseudopalisaded histiocytic reaction is a result of IL-6 inhibition in these patients. It will be interesting to see if the pattern of pseudopalisaded histiocytic hyperplasia becomes less frequent in postmortem samples following the routine use of dexamethasone rather than sarilumab in hospitalized patients requiring respiratory support.

Intriguingly, two patients dying of causes unrelated to COVID-19 tested positive for SARS-CoV-2 by PCR and serology but showed either no lung involvement, or in one case, limited pulmonary involvement (~5% of parenchyma) but with similar immunopathologic features of early exudative phase DAD. A concept of regional alveolar damage (RAD) was proposed three decades ago to describe such histologic findings; however, patients with RAD all developed respiratory failure, with 9 of the 10 patients requiring mechanical ventilation [32]. Our single patient showing regional alveolar damage, as well as the other patient without such findings, both tested positive by RT-PCR at admission and prior to death and also showed evidence of immune response with Sars-CoV-2 IgG and IgM antibodies detected in serum prior to death. Thus, their findings cannot be merely explained as an early pre-symptomatic phase of infection. It remains unclear why some patients develop severe and fatal COVID-19 while others can be asymptomatic carriers. Advanced age and comorbid conditions (obesity, hypertension, diabetes, chronic heart, and kidney disease) are more frequent in fatal COVID cases. A subset of patients with severe/fatal disease has been linked to inborn errors in the type I interferon immune pathway [6], as well as the development of neutralizing autoantibodies against the type I interferons [7]. An association between immune variations and comorbid conditions has also been proposed [33].

Aside from DAD, much attention has been given to the thrombosis associated with COVID-19 [16,34,35]. Microthrombi within the alveolus is a common finding in DAD from any etiology, and the frequency of this finding is likely proportional to the number of tissue sections sampled. We observed microthrombi in 60% of patients dying of COVID-19 and in 43% of non-SARS-CoV-2 associated DAD controls. Given that the number of tissue blocks sampled among the SARS-CoV-2 cases was 10-fold greater than the non-SARS-CoV-2 controls, this mild difference may not be significant. A similar frequency of pulmonary microthrombi between cases of DAD related and unrelated to COVID-19 has been reported in another autopsy series as well [36]. Conversely, macrothrombi were observed in 40% of COVID-19 associated DAD but not in the asymptomatic SARS-CoV-2 cases or non-COVID-19 DAD controls. This finding is in keeping with other large COVID-19 autopsy studies in which large vessel thrombi were observed in 20−42% of cases [11,13]. In our series, macrothrombi were observed more frequently in those dying in the fourth to fifth week from symptom onset (third to the fourth week of ventilation), usually in association with pseudopalisaded histiocytic hyperplasia and/or proliferative phase DAD as compared to microthrombi that were observed in all phases of DAD. Similar observations of the timing of macrothrombi were seen in a larger multi-institutional autopsy cohort [13], and a clinical cohort, where those not improving on mechanical ventilation were evaluated by pulmonary angiography [34]. Consistent with clinical studies, we observed macrothrombi in those with the highest D-dimer values [35]. The specifics of COVID-

19-induced coagulopathy remain complex with cytokine-induced overexpression of tissue factor, endothelial dysfunction leading to loss of antithrombotic phenotype, and overall hypoxia and stasis being the leading mechanistic hypothesis [37]. What is clear is that the degree of inflammation appears to correlate strongly with coagulopathy, with D-dimer levels showing a strong correlation with other inflammatory markers such as CRP, ESR, ferritin, and procalcitonin [35]. It is possible that the pseudopalisaded histiocytic hyperplasia is a marker of an inflammatory disease-prone phase to accentuate the coagulopathy of COVID-19. Of note, inflammation-associated coagulopathy is not specific to SARS-CoV-2 as it has also been described in critically ill patients with H1N1 and SARS-CoV-1 [38]. Randomized control trials to determine the optimal use of anticoagulation in COVID-19 patients are ongoing.

Several limitations must be considered in the interpretation of our findings. First, our sample size in both COVID-19 and the non-COVID-19 control cases is small. Second, the control group suffered from a variety of immune disorders (cancer, AIDS, autoimmune diseases), which were not frequent in our COVID-19 cases. Third, the control cases in our series were a median of two decades younger than our COVID-19 cases, and thus, we cannot assess the role of age-related immunosenescence contributing to the immunopathology in our COVID-19 cohort. Finally, as already stated, we cannot exclude that IL-6 inhibition due to treatment with sarilumab resulted in the pseudopalisaded histiocytic reaction.

5. Conclusion

COVID-19 associated DAD is associated with a unique pseudopalisaded histiocytic hyperplasia interposed between the early and proliferative phase, most pronounced at the fourth week from symptom onset (third week of ventilation). This unique inflammatory pattern may represent the immunopathology behind dexamethasone-induced mortality benefit. Pulmonary macrothrombi were seen predominantly in the proliferative phase of the disease and were associated with the highest D-Dimer levels. Asymptomatic SARS-CoV-2 infection may cause similar immunopathologic features in the lung but with a more limited tissue distribution.

References

[1] COVID-19 Map - Johns Hopkins Coronavirus Resource Center. https://coronavirus.jhu.edu/map.html (Accessed May 8, 2021).

[2] Arons MM, Hatfield KM, Reddy SC, Kimball A, James A, Jacobs JR, et al. Presymptomatic SARS-CoV-2 infections and transmission in a skilled nursing facility. N Engl J Med 2020;382:2081−90. https://doi.org/10.1056/NEJMoa2008457.

[3] Li H, Liu L, Zhang D, Xu J, Dai H, Tang N, et al. SARS-CoV-2 and viral sepsis: observations and hypotheses. Lancet Lond Engl 2020; 395:1517−20. https://doi.org/10.1016/S0140-6736(20)30920-X.

[4] Mehta P, McAuley DF, Brown M, Sanchez E, Tattersall RS, Manson JJ. COVID-19: consider cytokine storm syndromes and immunosuppression. Lancet 2020;395:1033−4. https://doi.org/10.1016/S0140-6736(20)30628-0.

[5] Prilutskiy A, Kritselis M, Shevtsov A, Yambayev I, Vadlamudi C, Zhao Q, et al. SARS-CoV-2 infection−associated hemophagocytic lymphohistiocytosis. Am J Clin Pathol 2020;154:466−74. https://doi.org/10.1093/ajcp/aqaa124.

[6] Zhang Q, Bastard P, Liu Z, Le Pen J, Moncada-Velez M, Chen J, et al. Inborn errors of type I IFN immunity in patients with life-threatening COVID-19. Science 2020;370:eabd4570. https://doi.org/10.1126/science.abd4570.

[7] Bastard P, Rosen LB, Zhang Q, Michailidis E, Hoffmann H-H, Zhang Y, et al. Autoantibodies against type I IFNs in patients with life-threatening COVID-19. Science 2020;370:eabd4585. https://doi.org/10.1126/science.abd4585.

[8] RECOVERY Collaborative Group, Horby P, Lim WS, Emberson JR, Mafham M, Bell JL, et al. Dexamethasone in hospitalized patients with covid-19 - preliminary report. N Engl J Med 2021;384: 693−704. https://doi.org/10.1056/NEJMoa2021436.

[9] Xu Z, Shi L, Wang Y, Zhang J, Huang L, Zhang C, et al. Pathological findings of COVID-19 associated with acute respiratory distress syndrome. Lancet Respir Med 2020;8:420−2. https://doi.org/10.1016/S2213-2600(20)30076-X.

[10] Barton LM, Duval EJ, Stroberg E, Ghosh S, Mukhopadhyay S. COVID-19 autopsies, Oklahoma, USA. Am J Clin Pathol 2020;153: 725−33. https://doi.org/10.1093/ajcp/aqaa062.

[11] Edler C, Schröder AS, Aepfelbacher M, Fitzek A, Heinemann A, Heinrich F, et al. Dying with SARS-CoV-2 infection-an autopsy study of the first consecutive 80 cases in Hamburg, Germany. Int J Legal Med 2020;134:1275−84. https://doi.org/10.1007/s00414-020-02317-w.

[12] Carsana L, Sonzogni A, Nasr A, Rossi RS, Pellegrinelli A, Zerbi P, et al. Pulmonary post-mortem findings in a series of COVID-19 cases from northern Italy: a two-centre descriptive study. Lancet Infect Dis 2020;20:1135−40. https://doi.org/10.1016/S1473-3099(20)30434-5.

[13] Borczuk AC, Salvatore SP, Seshan SV, Patel SS, Bussel JB, Mostyka M, et al. COVID-19 pulmonary pathology: a multi-institutional autopsy cohort from Italy and New York City. Mod Pathol Off J U S Can Acad Pathol Inc 2020;33:2156−68. https://doi.org/10.1038/s41379-020-00661-1.

[14] Tian S, Hu W, Niu L, Liu H, Xu H, Xiao S-Y. Pulmonary pathology of early-phase 2019 novel coronavirus (COVID-19) pneumonia in two patients with lung cancer. J Thorac Oncol 2020;15:700−4. https://doi.org/10.1016/j.jtho.2020.02.010.

[15] Tian S, Xiong Y, Liu H, Niu L, Guo J, Liao M, et al. Pathological study of the 2019 novel coronavirus disease (COVID-19) through postmortem core biopsies. Mod Pathol 2020;33:1007−14. https://doi.org/10.1038/s41379-020-0536-x.

[16] Ackermann M, Verleden SE, Kuehnel M, Haverich A, Welte T, Laenger F, et al. Pulmonary vascular endothelialitis, thrombosis, and angiogenesis in covid-19. N Engl J Med 2020;383:120−8. https://doi.org/10.1056/NEJMoa2015432.

[17] Wichmann D, Sperhake J-P, Lütgehetmann M, Steurer S, Edler C, Heinemann A, et al. Autopsy findings and venous thromboembolism in patients with COVID-19: a prospective cohort study. Ann Intern Med 2020;173:268−77. https://doi.org/10.7326/M20-2003.

[18] Polak SB, Van Gool IC, Cohen D, von der Thüsen JH, van Paassen J. A systematic review of pathological findings in COVID-19: a pathophysiological timeline and possible mechanisms of disease progression. Mod Pathol Off J U S Can Acad Pathol Inc 2020;33: 2128−38. https://doi.org/10.1038/s41379-020-0603-3.

[19] Schaefer I-M, Padera RF, Solomon IH, Kanjilal S, Hammer MM, Hornick JL, et al. In situ detection of SARS-CoV-2 in lungs and airways of patients with COVID-19. Mod Pathol Off J U S Can Acad Pathol Inc 2020;33:2104−14. https://doi.org/10.1038/s41379-020-0595-z.

[20] Nienhold R, Ciani Y, Koelzer VH, Tzankov A, Haslbauer JD, Menter T, et al. Two distinct immunopathological profiles in autopsy

lungs of COVID-19. Nat Commun 2020;11:5086. https://doi.org/10.1038/s41467-020-18854-2.
[21] Sweeney RM, McAuley DF. Acute respiratory distress syndrome. Lancet Lond Engl 2016;388:2416−30. https://doi.org/10.1016/S0140-6736(16)00578-X.
[22] Tomashefski JF. Pulmonary pathology of acute respiratory distress syndrome. Clin Chest Med 2000;21:435−66. https://doi.org/10.1016/s0272-5231(05)70158-1.
[23] Rendeiro AF, Ravichandran H, Bram Y, Salvatore S, Borczuk A, Elemento O, et al. The spatio-temporal landscape of lung pathology in SARS-CoV-2 infection. MedRxiv Prepr Serv Health Sci 2020. https://doi.org/10.1101/2020.10.26.20219584.
[24] Katzenstein AL. Pathogenesis of "fibrosis" in interstitial pneumonia: an electron microscopic study. Hum Pathol 1985;16:1015−24. https://doi.org/10.1016/s0046-8177(85)80279-3.
[25] Annane D, Pastores SM, Rochwerg B, Arlt W, Balk RA, Beishuizen A, et al. Guidelines for the diagnosis and management of critical illness-related corticosteroid insufficiency (CIRCI) in critically ill patients (Part I): society of Critical Care Medicine (SCCM) and European Society of Intensive Care Medicine (ESICM) 2017. Intensive Care Med 2017;43:1751−63. https://doi.org/10.1007/s00134-017-4919-5.
[26] Steinberg KP, Hudson LD, Goodman RB, Hough CL, Lanken PN, Hyzy R, et al. Efficacy and safety of corticosteroids for persistent acute respiratory distress syndrome. N Engl J Med 2006;354:1671−84. https://doi.org/10.1056/NEJMoa051693.
[27] Rodrigo C, Leonardi-Bee J, Nguyen-Van-Tam J, Lim WS. Corticosteroids as adjunctive therapy in the treatment of influenza. Cochrane Database Syst Rev 2016;3:CD010406. https://doi.org/10.1002/14651858.CD010406.pub2.
[28] Lansbury L, Rodrigo C, Leonardi-Bee J, Nguyen-Van-Tam J, Lim WS. Corticosteroids as adjunctive therapy in the treatment of influenza. Cochrane Database Syst Rev 2019;2:CD010406. https://doi.org/10.1002/14651858.CD010406.pub3.
[29] Chaudhuri D, Sasaki K, Karkar A, Sharif S, Lewis K, Mammen MJ, et al. Corticosteroids in COVID-19 and non-COVID-19 ARDS: a systematic review and meta-analysis. Intensive Care Med 2021;47:521−37. https://doi.org/10.1007/s00134-021-06394-2.
[30] Khiali S, Rezagholizadeh A, Entezari-Maleki T. A comprehensive review on sarilumab in COVID-19. Expert Opin Biol Ther 2021;21:615−26. https://doi.org/10.1080/14712598.2021.1847269.
[31] Hoge J, Yan I, Jänner N, Schumacher V, Chalaris A, Steinmetz OM, et al. IL-6 controls the innate immune response against Listeria monocytogenes via classical IL-6 signaling. J Immunol Baltim Md 1950 2013;190:703−11. https://doi.org/10.4049/jimmunol.1201044.
[32] Yazdy AM, Tomashefski JF, Yagan R, Kleinerman J. Regional alveolar damage (RAD). A localized counterpart of diffuse alveolar damage. Am J Clin Pathol 1989;92:10−5. https://doi.org/10.1093/ajcp/92.1.10.
[33] Trump S, Lukassen S, Anker MS, Chua RL, Liebig J, Thürmann L, et al. Hypertension delays viral clearance and exacerbates airway hyperinflammation in patients with COVID-19. Nat Biotechnol 2020. https://doi.org/10.1038/s41587-020-00796-1.
[34] Klok FA, Kruip MJHA, van der Meer NJM, Arbous MS, Gommers D, Kant KM, et al. Confirmation of the high cumulative incidence of thrombotic complications in critically ill ICU patients with COVID-19: an updated analysis. Thromb Res 2020;191:148−50. https://doi.org/10.1016/j.thromres.2020.04.041.
[35] Al-Samkari H, Karp Leaf RS, Dzik WH, Carlson JCT, Fogerty AE, Waheed A, et al. COVID-19 and coagulation: bleeding and thrombotic manifestations of SARS-CoV-2 infection. Blood 2020;136:489−500. https://doi.org/10.1182/blood.2020006520.
[36] Konopka KE, Nguyen T, Jentzen JM, Rayes O, Schmidt CJ, Wilson AM, et al. Diffuse alveolar damage (DAD) resulting from coronavirus disease 2019 Infection is Morphologically Indistinguishable from Other Causes of DAD. Histopathology 2020;77:570−8. https://doi.org/10.1111/his.14180.
[37] Chan NC, Weitz JI. COVID-19 coagulopathy, thrombosis, and bleeding. Blood 2020;136:381−3. https://doi.org/10.1182/blood.2020007335.
[38] Goeijenbier M, van Wissen M, van de Weg C, Jong E, Gerdes VEA, Meijers JCM, et al. Review: viral infections and mechanisms of thrombosis and bleeding. J Med Virol 2012;84:1680−96. https://doi.org/10.1002/jmv.23354.